ELSEVIER

Earth and Planetary Science Letters 195 (2002) 131–139

EPSL

www.elsevier.com/locate/epsl

Does the calculated decay constant for ^{7}Be vary significantly with chemical form and/or applied pressure?

J.A. Tossell *

Department of Chemistry and Biochemistry, University of Maryland, College Park, MD 20742, USA

Received 17 July 2001; received in revised form 7 September 2001; accepted 26 October 2001

Abstract

It has recently been reported that the electron capture decay constant for ^{7}Be varies by as much as 1.5% in different oxidic compounds of Be and that application of 400 kbar pressure to a $Be(OH)_2$ gel increases its ^{7}Be decay constant by about 1%. Differences of such magnitude in decay rate might be useful in determining the speciation of Be in glasses, gels and aqueous solutions. We have recently calculated structures, ^{9}Be NMR shieldings and IR/Raman spectra for both monomeric and oligomeric species of Be to assist in determining Be speciation. We here use similar methods to calculate the electron densities at the Be nucleus, which determine the rates of electron capture decay. We find that variations in the electron density at the Be nucleus in a number of oxidic compounds are only at the 0.1–0.4% level, as had been concluded in the 1970s. This raises doubts about the recent experimental results which show larger variations from one oxidic compound to another. The calculated ^{9}Be NMR shifts of these species differ by only a few ppm, but such changes are readily measurable by NMR spectroscopy, and they depend systematically on the degree of hydrolysis and the degree of oligomerization. Rough estimates of the effects of Be–O bond compression in $Be(OH)_4^{2-}$ on the energy and the electron density at the nucleus indicate that several hundred kbar of pressure could increase the electron density by 1% or more, qualitatively consistent with the experimental results.

Keywords: Be-7; radioactive decay; high pressure; electrons

1. Introduction

The suggestion was first made in the 1940s that nuclei which decay by electron capture might show observable changes in their decay constants as a result of chemical combination [1]. The most important nucleus decaying by electron capture is probably ^{40}K, since it is important in the radioactive dating of many earth materials due to its ubiquitous presence and long half-life. However, theoretical studies on the electron density at the K nucleus at high pressure in K metal established that the density variation was too small to be observable – the maximum calculated change in decay constant was about three orders of magnitude smaller than the uncertainty in its measurement [2]. ^{7}Be also undergoes electron capture decay. Since it has a much smaller ratio of number

* Tel.: +1-301-405-1868; Fax: +1-301-314-9121.
E-mail address: tossell@chem.umd.edu (J.A. Tossell).

0012-821X/02/$ – see front matter
PII: S0012-821X(01)00569-6

of core s electrons to number of valence s electrons it could conceivably show a much larger percent variation in electron density at the nucleus. Recently new values have been reported for the half-life of ^{7}Be electron capture decay in a range of oxidic materials, which apparently show variations up to 1.5% [3,4]. The same researchers have reported increases at the 1% level in the ^{7}Be decay constant for $Be(OH)_2$ gel exposed to pressures up to 400 kbar [5]. Changes of this order of magnitude in the decay constant might reduce the utility of ^{7}Be as a probe of Be movement within geochemical environments, such as estuaries [6]. Such a large variation in ^{7}Be decay constant was unexpected since studies as late as the mid-1990s [7], although based partly on rather unsystematic studies on various Be compounds in the 1970s [8,9], indicated that the effects of chemical combination on the decay constants were at the 0.1% level, roughly an order of magnitude smaller than the recent results. It was also concluded in [7] that the magnitudes of errors in the decay constants were generally underestimated, since discrepancies between different labs were uniformly larger than their reported standard errors. Similarly, studies of the decay of ^{7}Be in crystalline BeO at pressures up to 270 kbar showed an increase of only about 0.5% in the decay constant [10].

We have recently reported calculated ^{9}Be NMR shifts for a number of different compounds [11,12], to help in the determination of Be speciation in solution. Accurate experimental and calculated NMR shieldings have recently been reported for a solid Be oxidic compound, bis(2,4-pentanedionato-O,O′)Be (also known as $Be(acac)_2$) [13]. In our study of Be aquo, hydroxo and oxo compounds we found systematic changes in the Be NMR shift as a function of both extent of hydrolysis (or ligand protonation state) and degree of oligomerization. Briefly, deprotonation of the oxidic ligand (e.g. transformation of $-OH_2$ to OH^-) *deshields* the Be, while oligomerization (e.g. transformation of $Be(OH)_4^{2-}$ to $Be_4(OH)_{10}^{2-}$, with loss of water) *shields* the Be. Since the most stable species in solution are deprotonated oligomers, their shieldings differ only slightly from that of the reference compound $Be(H_2O)_4^{2+}$, but these differences can be measured very accurately. For metallic elements like Be or Na [14] there is some correlation of NMR shieldings with ground state charge distributions, within a series of similar compounds, with the magnitude of the paramagnetic deshielding increasing with the amount of electron density transferred to the metal atom by its ligands.

There is substantial interest in determining the local environments of Be in minerals [15] and the speciation of Be in solution [16], but few methods exist for making such determinations. It is known that Be^{2+}, like Al^{3+}, forms a number of aquo, hydroxide and oxide species in solution, both monomeric and oligomeric. Sorting out the detailed speciation of Be is difficult, relying upon solubility studies and on spectral data, mainly from vibrational and NMR spectra. It is thought that the toxicity of Be in solution may be affected by changes in its speciation. Although ^{9}Be NMR is becoming increasing powerful in determining Be speciation it is still limited by the quadrupolar nature of the nuclide and the consequent breadth of its NMR lines. It would certainly be desirable to have an additional experimental probe of local geometry about the Be. The electron capture decay rate of ^{7}Be could be such a probe if it changes measurably from one compound to another, particularly if this change depends systematically on extent of hydrolysis, degree of polymerization, etc. In this study we calculate the electron density at the Be nucleus in a number of different compounds, trying to establish the magnitude of the change in this property and its systematic dependence upon local structural properties.

As explained in [2] the nuclear reaction my be approximated as:

$$p + e^- \Rightarrow n + \nu \quad (1)$$

where p, e^-, n and ν are the proton, electron, neutral and gamma ray photon, respectively. Assuming the nuclear wavefunctions are unaffected by chemical combination or pressure the change in the rate of electron capture decay, $\delta\lambda_e$, for a compound A with respect to some reference compound can be represented as:

$$\delta\lambda_e = (\rho_{Be\,A}/\rho_{Be\,ref} - 1)\lambda_{ref} \quad (2)$$

where ρ is the electron density at the Be nucleus. Thus the relevant theoretical quantity is the ratio of the electron densities at the Be nucleus minus 1.

2. Computational methods

To evaluate the electron density at the Be nucleus and other properties of the Be compounds we carried out Hartree–Fock, Moller–Plesset second-order (MP2) and hybrid HF density functional generalized gradient approximation (B3LYP)) calculations [17] on a number of model molecules. We used standard 6-31G* (polarized, double-zeta) basis sets [18] and the software packages GAMESS [19] to calculate equilibrium structures and energies, and densities and electric field gradients at the Be nucleus. The Be NMR shieldings were calculated with GAUSSIAN94 [20] using the GIAO method [21] and 6-31G* basis sets. We also calculated the electron density at the Be nucleus using both GAMESS and GAUSSIAN94 with a range of larger, more flexible basis sets, up to the polarized triple zeta plus diffuse (TZVP+ [22]) and the EPR-III [23] basis sets. In general, we expect, according to the quantum mechanical Variational Principle, that using larger basis sets for the expansion of the molecular orbitals will give a more accurate solution of the HF equation, producing more accurate total energies and also more accurate electron densities at the nucleus. The number of s contracted Gaussians (only s orbitals give nonzero densities at the nucleus) increases in the series 3, 5, 6 and 7 for the series of basis sets 6-31G*, 6-311+G(2d,p), TZVP+ and EPR-III. The EPR-III bases have additional 'tight' s orbitals and are specifically designed to obtain accurate densities of unpaired spin electrons at the nucleus in density functional theory calculations of hyperfine coupling constants. However, using larger basis sets greatly increases the difficulty of the computation, since the computer time required scales as a high power of the size of the basis set, usually around the fourth power. For the larger molecules considered we have used mainly 6-31G* basis sets because they require much less computer time than the larger basis sets. For example, in the interesting polyhedral oligomer $Be_4(OH)_{10}^{2-}$, calculating the wavefunction and density at the nucleus required 15 min for the 6-31G* basis set (with a total of 230 basis functions) and 360 min for the TZVP+ basis set (with a total of 396 basis functions). As will be seen in Section 3, the 6-31G* basis set results seem to systematically show a larger change in density at the nucleus than the results using the larger basis sets. Therefore by using the 6-31G* basis we are obtaining an upper bound on the magnitude of the density variation.

One serious concern in using such methodologies is that they are all based on Gaussian-type orbitals (GTOs), which do not show the discontinuity in the gradient of the wavefunction at the nucleus (the 'cusp') which is found both in accurate atomic orbitals and in simple Slater-type orbitals (STOs). However, studies by Nakatsuji and Izawa [25] have indicated that conventional basis sets comprised of sufficiently large and flexible sets of GTOs can give quite accurate values for properties which depend upon the electron density at the nucleus, e.g. the nuclear hyperfine splitting constants, even when they give poor numerical values for the cusp. In any case, very few quantum mechanical programs presently can utilize STOs, since GTOs are much more efficient for molecular computations.

We choose a molecular approach since our main interest is in species in solutions and glasses, which do not possess long range order. For crystalline materials one could utilize a band theoretical approach, such as was applied in [2] to crystalline K. However, such methods have their own difficulties – most all-electron band methods require the choice of sphere radii centered on the nuclei and the radius chosen can slightly modify the electron density calculated at the nucleus.

In most cases the geometries of the species considered have been optimized at the 6-31G* Hartree–Fock level. Pictures of many of the species considered are given in [12]. In some cases cluster models of crystalline solids were extracted from experimental crystal structures using CrystalMaker software [24].

3. Results

We first calculated the electron density at the Be nucleus for the two small molecules $Be(H_2O)_4^{2+}$ and $Be(OH)_4^{2-}$, generally using geometries optimized at the 6-31G* HF level. We also tested the effect of using larger basis sets in the geometry optimizations. To evaluate the electron density at the nucleus we employed a number of different basis sets, ranging in size from the fairly small 6-31G* basis to the very large basis EPR-III, and employed Hartree–Fock, MP2 and B3LYP methods. The density at the Be nucleus for each species increased as the basis set became more flexible but decreased when electron correlation was introduced using the MP2 or B3LYP methods. However, the change from the TZVP+ basis to the EPR-III basis was much smaller than the change from 6-31G* to TZVP+. Similarly the effects of correlation, as calculated by MP2 or B3LYP methods, were fairly small.

The most important quantity for describing the variation in decay constant from one compound to another is the relative % increase in density which we label in Table 1 as (ratio−1.0)×100%.

This is defined as: $(\rho_{Be\ A}/\rho^{2+}_{Be\ Be(H2O)4}-1.0)\times 100\%$ and gives the excess electron density at Be in the sample environment A compared to that in $Be(H_2O)_4^{2+}$. We choose $Be(H_2O)_4^{2+}$ as our reference since it is the predominant Be^{2+} species in water at low pH and in Be NMR reference solutions such as $Be(NO_3)_2$ (aq). We see that the relative % increase for $Be(OH)_4^{2-}$ vs. $Be(H_2O)_4^{2+}$ has a value around 0.2% using the 6-31G* basis and 6-31G* geometries and values somewhat below 0.1% for *all* the larger bases, and for Hartree–Fock, MP2 and B3LYP methods (at the 6-31G* geometries). The relative % increase is also less than 0.1% if we employ the same large basis sets (6-311+G(2d,p) or TZVP+) to both optimize the geometry and evaluate the electron density.

If the accuracy in determination of the decay constant is indeed at the 0.01% level as quoted in [3] we should be able to reliably distinguish between the $Be(H_2O)_4^{2+}$ and $Be(OH)_4^{2-}$ species based on electron density at the nucleus and decay constant. They can also be easily distinguished by NMR since their shift difference is a few ppm (see Table 2), which is easily measurable. As we will see below, however, it is not certain that such experimental accuracy in the decay constants is really attainable.

The simplest way of explaining the difference in density at the Be nucleus in these two compounds is in terms of the overall charge distribution. Using 6-31G* optimized geometries and 6-31G* basis sets the Mulliken charge (a simple approximation to the charge distribution obtained from the molecular orbital coefficients) on Be in $Be(H_2O)_4^{2+}$ is +0.94 charge units while that on Be in $Be(OH)_4^{2-}$ is only +0.63 charge units, i.e. the valence electron density on Be is larger in $Be(OH)_4^{2-}$, which is consistent with a larger electron density at the nucleus. However, there are compensating effects from the 1s core which we discuss further below (see Table 3).

In Table 2 we show results for the electron density, the relative % increase in electron density with respect to $Be(H_2O)_4^{2+}$ and various NMR

Table 1
Electron densities (in electrons au^{-3}) calculated for $Be(OH)_4^{2-}$ and $Be(OH_2)_4^{2+}$ at their 6-31G* optimized geometries, as a function of basis set and method, with some results for geometries optimized with larger basis sets in parentheses

Method	Basis	ρ_{Be} $Be(OH)_4^{2-}$	$\rho_{Be}Be(OH_2)_4^{2+}$	(Ratio−1)×100%
HF	6-31G*	32.6908	32.6261	0.198
HF	6-311+G(2d,p)	32.8183 (32.8153)	32.7918 (32.8064)	0.081 (0.027)
HF	TZVP+	33.4660 (33.4634)	33.4464 (33.4509)	0.059 (0.034)
HF	EPR-III	33.7392	33.7188	0.061
B3LYP	6-311+G(2d,p)	32.9140	32.8901	0.073
MP2	6-311+G(2d,p)	32.8354	32.8065	0.088
B3LYP	EPR-III	34.0627	34.0389	0.070
MP2	EPR-III	33.7621	33.7340	0.083

Table 2
Electron densities (in electrons au^{-3}) and density variations vs. $Be(OH_2)_4^{2+}$ (calculated at the 6-31G* level with 6-31G* optimized geometries) for a number of Be compounds, compared with calculated Be NMR shieldings and shifts

Molecule	ρ_{Be}	(Ratio−1)×100%	σ^{Be} (ppm)	δ^{Be} (ppm)
$Be(OH_2)_4^{2+}$	32.6261	0	120.1	
$Be(OH)_4^{2-}$	32.6908	0.198	117.6	2.5
		0.51		
$Be_2(OH)_7^{3-}$	32.6703	0.135	117.3	2.8
				2.1
$Be_3(OH)_3(OH_2)_6^{3+}$	32.6630	0.113	119.2	0.9
				0.61
$Be_3(OH)_9^{3-}$	32.6775	0.157	118.1	2.0
$Be_3O_3(OH_2)_6$	32.7405	0.351	113.7	6.4
$Be_4(OH)_{10}^{2-}$	32.7242	0.301	117.8	2.3
	3×32.7163	0.276	3×117.6	2.5
				2.0
$Be_6(OH)_9(OH_2)_6^{3+}$	32.6607	0.106	118.2	1.9
BeO model $Be_{12}O_{13}^{2-}$ at X-ray geom.	32.6558	0.091	118.2	1.9
		−0.037, −0.992		
Model for $Be(OH)_2Be_{10}H_{13}O_{17}^{1-}$ at X-ray geom.	32.7118	0.263	122.0	−1.9
		0.51		
$Be_4O(CH_3CO_2)_6$				
at X-ray geom.	32.6800	0.165	117.6–117.8	2.5–2.3
at opt. geom.	32.6539	0.085	117.6–117.9	2.2–2 5
		0.035		
$Be(C_3O_4H_2)_2^{2-}$	32.6716	0.139	115.9	4.2
$Be_3(OH)_3(C_3O_4H_2)_3^{3-}$	32.6774	0.157	117.4	2.7
$Be(CH_3)_2$	33.0184	1.202	90.1	30.0
C_5H_5BeCl	32.6067	−0.059	137.2	−17.1
				−19.1

Experimental decay constant ratios from [3] and [9] and experimental NMR shifts (quoted in [13]) are given in bold.

properties, all determined at the 6-31G* Hartree–Fock level, for a number of compounds. The cluster models used for $Be(OH)_2$ and basic Be acetate solids are shown in Fig. 1. The relative % increases for all the oxidic compounds in Table 2 are at the 0.4% level or lower. Our calculations on a limited number of these species using larger basis sets also indicate that the larger basis sets give smaller relative % increases in density, e.g. the relative % increases in electron density for the different Be atoms of $Be_4(OH)_{10}^{2-}$ drop from about 0.33% at the 6-31G* level to about 0.14% at the TZVP+ basis set level.

However, if we consider a wider range of Be compounds the relative % increases do have somewhat larger magnitudes. For example, one of the Be compounds most highly shielded in NMR, C_5H_5BeCl, and one of the least shielded, $(CH_3)_2Be$, differ by about 1.8% in density at the Be nucleus (Table 2). Study of such compounds might give a more definitive determination of the variation in electron density at Be and the ^7Be decay constant.

There appear to be some systematics in the changes in density at the Be nucleus for the different oxidic species shown in Table 2. As we deprotonate the oxidic ligands the density at the Be nucleus clearly increases. There is also a trend toward larger electron density in the *cage* oligomers, such as $Be_4(OH)_{10}^{2-}$, although not in the ring oligomers. Thus the effects of deprotonation and oligomerization are in some cases additive, while for NMR shieldings they oppose each other [11,12]. Therefore the decay constants and NMR shieldings would give complementary information on speciation. The effects of two OH^- ligands and a single bidentate malonate, $C_3O_4H_2^{2-}$, ligand on the electron density at the Be seem to be fairly

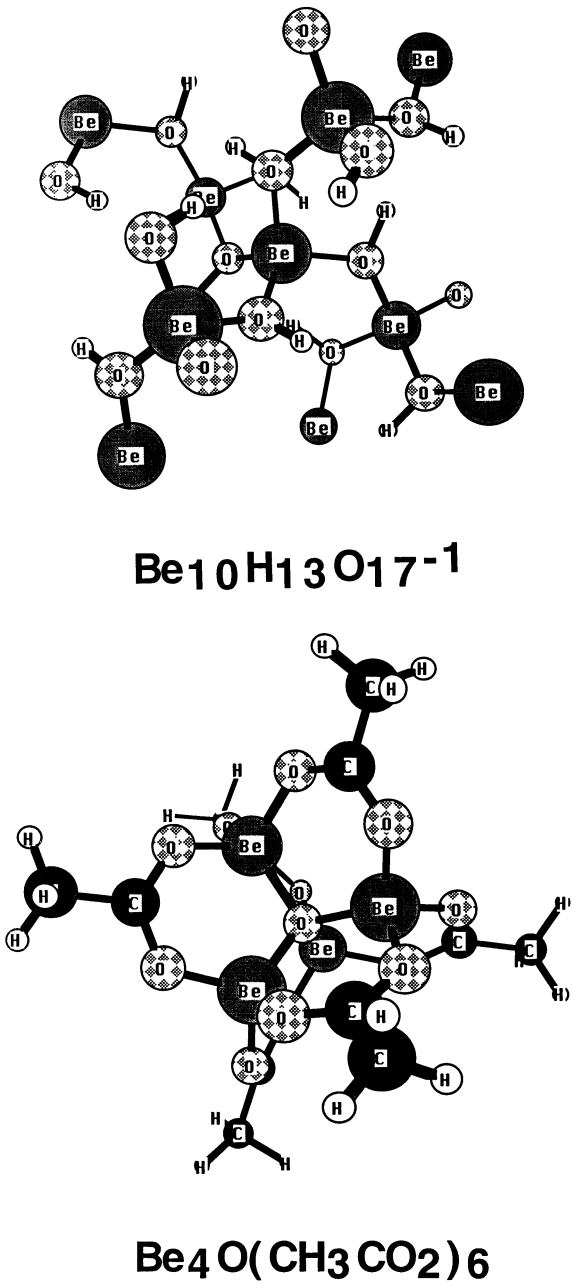

Fig. 1. Structures for the $Be_{10}H_{13}O_{17}^{1-}$ model used for $Be(OH)_2$(s) and for $Be_4O(CH_3CO_2)_6$ (basic beryllium acetate).

similar. It therefore seems that highly accurate measurement of the ^{7}Be decay constant might be useful in addressing some, but by no means all, questions concerning Be speciation.

Only limited comparisons can be made with experiment since in most cases the experimental determinations have been made on solids which were precipitated from solution and not well characterized crystallographically (a problem which is common in such nuclear chemical studies) or on poorly defined aqueous species. The earlier literature [9] reports a 0.51% difference between $Be(OH)_4^{2-}$ and $Be(H_2O)_4^{2+}$, which is considerably larger than our value of 0.198% obtained at the 6-31G* Hartree–Fock level or 0.070 obtained at the EPR-III BLYP level. Values have also been reported for solids characterized as $Be(OH)_2$ and BeO but the values are not consistent from one report to another. The most recent study [3] gives −0.992% for BeO while a study from the 1970s gives −0.037%. Using CrystalMaker and the reported crystal structure [26] we have created a $Be_{12}O_{13}^{2-}$ cluster model for BeO which gives a relative % density increase of +0.091%, in the opposite direction to experiment. Attempts to calculate an equilibrium geometry at the 6-31G* Hartree–Fock level starting with this structure give Be–O distances that were inequivalent by a large amount and differed by more than 0.1 Å from the experimental values. Such a reoptimization of the structure would certainly be desirable since our reference molecule $Be(H_2O)_4^{2+}$ is treated at its calculated 6-31G* HF equilibrium geometry and comparing a calculated geometry for one material with an experimental geometry for another may well introduce artifacts. Of course it is also not obvious that the 'BeO' studied experimentally actually corresponds to the crystalline material. A $Be_{10}H_{13}O_{17}^{1-}$ model has been constructed for $Be(OH)_2$ from its structural data [27] using CrystalMaker and its calculated electron density is qualitatively consistent with that reported experimentally (+0.263% calculated and 0.51% experimental) but again we were unable to obtain an optimized geometry which seemed consistent with the experimental bond distances. For basic Be acetate [28], which is essentially a molecular solid, we were able to abstract a neutral molecule $Be_4O(CH_3CO_2)_6$ from the crystal structure and to optimize its structure, resulting in bond distances in good agreement with experiment. The calculated relative electron density increases were

Table 3
Core and valence contributions to electron density at the nucleus in $Be(OH_2)_4^{2+}$, $Be(OH)_4^{2-}$ and $Be_4(OH)_{10}^{2-}$, using TZVP+ basis sets

Molecule	Core electron density	Valence electron density	Total electron density	Mulliken charge on Be
$Be(OH_2)_4^{2+}$	32.9090	0.5374	33.4464	1.044
$Be(OH)_4^{2-}$	32.8986	0.5674	33.4660	1.011
$Be_4(OH)_{10}^{2-}$	32.8770	0.6152	33.4922	0.702

0.165% and 0.085% at the experimental and optimized structures, while the single experimental report from the 1970s gives 0.035%. No experimental results are available for other Be compounds which we calculate to show larger electron density effects, such as the strongly deshielded $(CH_3)_2Be$ and shielded C_5H_5BeCl. As noted before, it would be highly desirable to measure the decay constants for Be in these compounds to match against our calculations.

To understand why the electron densities at the Be nucleus show relatively little variation it is instructive to separate the contributions of the Be $1s^2$ core electrons from that for the valence electrons, as shown in Table 3 for $Be(OH_2)_4^{2+}$, $Be(OH)_4^{2-}$ and $Be_4(OH)_{10}^{2-}$, using TZVP+ basis sets. The results in Table 3 show that the less positive the Mulliken charge on the Be the *larger* the valence electron contribution to the electron density at the Be nucleus. However, less positive Mulliken charges are also associated with less contraction of the $1s^2$ shell and consequently with a *smaller* core contribution to the electron density at Be. The valence and core effects thus oppose each other, so that the total electron density at the Be nucleus shows little change from one compound to another.

Finally, we have calculated the change in electron density at Be in $Be(OH)_4^{2-}$ (using the TZVP+ basis and the HF method) as a very *simple* model for a $Be(OH)_2$ gel, at a series of different Be–O distances and have estimated the pressures required to produce such shortenings. Since the molecule considered is a small one, calculations with the TZVP+ basis set are feasible for a range of geometries. In Table 4 we show results for 1, 5, 10 and 20% shortening of the Be–O bond, with the stronger O–H bond *assumed* constant in length. For a 20% shortening the relative % increase in electron density is 1.33%. For this Be–O bond distance the energy of the $Be(OH)_4^{2-}$ ion has increased by 603.8 kJ/mol and its volume has decreased by 2.68×10^{-5} m^3 (based on volumes calculated using GAUSSIAN94). The approximate pressure required to produce a given shortening corresponds to the slope of the plot of ΔE vs. volume at that volume. If we fit the ΔE vs. volume data to a third-order polynomial we find that the slope at 20% compression corresponds to a pressure of about 680 kbar. Therefore the calculated increase in electron density with pressure is of the order of magnitude observed (about 1% in 400 kbar). Of course this model for $Be(OH)_2$ gel is an extremely crude one but our results do suggest that such pressure effects should be observable. There is also a systematic NMR deshielding of

Table 4
Variation in the electron density at the Be nucleus in $Be(OH)_4^{2-}$, evaluated with the TZVP+ basis set, starting from the 6-31G* optimized geometry, along with total energy, energy difference, estimated volume and pressure and Be NMR shielding (evaluated at the 6-31G* level)

R(Be–O) (Å)	Percentage shortening	ρ_{Be}	(Ratio−1)×100%	ΔE (kJ/mol)	Volume ($\times10^{-5}$ m^3)	Pressure $=\Delta E/\Delta V$ (kbar)	σ^{Be} (ppm)
1.684	0	33.4660	0	0	5.49		117.6
1.667	1.0	33.4782	0.036	0.8	5.33	5.0	117.3
1.600	5.0	33.5347	0.205	23.6	4.71	30.3	116.6
1.515	10.0	33.6260	0.478	109.2	4.00	73.3	115.5
1.347	20.0	33.9116	1.332	603.8	2.81	225.3	113.2

the Be as the Be–O distance is reduced, which may be useful for estimating the Be–OH bond distance.

4. Sources of uncertainty in comparing calculated densities and experimental decay constants

There are two main uncertainties in comparing our calculated trends in densities with experimental trends in decay constants. The first concerns the quality of the calculations of electron density at the nucleus, particularly the effect of using Gaussian-type orbitals. At present we have evidence that Gaussian-type orbitals can accurately describe properties such as the spin density at the nucleus but no *direct* evidence that they give accurate total electron densities or trends in electron densities. The second concerns the actual identity of the samples studied experimentally and the adequacy of our molecular cluster representations of them. The samples are not generally characterized as crystalline materials – we know only their chemical composition. Therefore, even if the calculations were performed on crystalline materials of the given composition we would not necessarily be looking at the same materials experimentally and computationally. Since we have adopted a cluster model for these condensed phase materials there is also the question of how well that model represents this particular property of the crystal. As we have noted, such cluster models have been used with success for a number of local properties of such materials, e.g. the Be NMR shieldings in oxidic materials. In comparing properties of compounds using cluster models we also wish to work with comparable geometries, either geometries which are all obtained experimentally or those which are all obtained theoretically using the same method. Due to difficulty in constructing cluster models which would optimize to reasonable geometries for some of the compounds this has been difficult to do. Therefore our results are suggestive rather than definitive – they suggest that variations in ^{7}Be decay constants will be small and that great care will need to be taken in accurately measuring the decay constants and properly characterizing the samples.

5. Conclusion

Calculated electron densities at the Be nucleus in oxidic compounds of Be show variations at the level of a few tenths of a percent. If electron capture decay constants can now indeed be measured with an accuracy of 0.01% [3] it may be possible to determine the Be species present in minerals, glasses and aqueous solutions by measuring their decay constants. However, comparisons of decay constants measured in different laboratories indicate that experimental errors may be larger than those stated. Comparisons of calculated changes in electron density with experimental changes in decay constants usually, but not always, give at least qualitative agreement. Other, non-oxidic, compounds of Be show a larger variation in calculated electron density and it would be useful to measure their ^{7}Be decay constants to establish the reliability and reproducibility of the approach. For oxidic Be compounds the electron density at Be, and thus the decay constant, increases with deprotonation of the oxidic ligand (e.g. from $-OH_2$ to OH^- to $-O^{2-}$) and with formation of cage oligomers. Application of pressure shortens the bonds in $Be(OH)_4^{2-}$ and increases the electron density at the nucleus by an amount qualitatively consistent with recent experimental results on $Be(OH)_2$ gel.

Acknowledgements

This work was supported by NSF Grant EAR-0001031 and DOE Grant DE-FG02-94ER14467. Calculations using the EPR-III basis sets were performed using GAUSSIAN98 on the Carnegie Alpha Cluster, which is supported in part by NSF MRI Grant AST-9976645.*[BW]*

References

[1] E. Segre, Possibility of altering the decay rate of a radioactive substance, Phys. Rev. 71 (1947) 274–275.
[2] M.S.T. Bukowinski, Theoretical estimate of compressional changes of decay constant of K-40, Geophys. Res. Lett. 6 (1979) 697–699.

[3] C.A. Huh, Dependence of the decay rate of ^{7}Be on chemical forms, Earth Planet. Sci. Lett. 171 (1999) 325–328.
[4] R.A. Kerr, Tweaking the clock of radioactive decay, Science 286 (1999) 882–883.
[5] L.-G. Liu, C.-A. Huh, Effect of pressure on the decay rate of ^{7}Be, Earth Planet. Sci. Lett. 180 (2000) 163–167.
[6] J.E. Dibb, D.L. Rice, The geochemistry of beryllium-7 in Chesapeake Bay, Estuar. Coast. Shelf Sci. 28 (1989) 379–394.
[7] M. Jaeger, S. Wilmes, V. Kolle, G. Staudt, P. Mohr, Precision measurement of the half-life of 7Be, Phys. Rev. C 54 (1996) 423–424.
[8] C.M. Lederer, J.M. Hollander, I. Perlman, Table of Isotopes, 6th edn., Wiley, New York, 1973.
[9] H.W. Johlige, D.C. Aumann, H.-J. Born, Determination of the relative electron density at the Be nucleus in different chemical combinations, measured as changes in the electron-capture half-life of 7Be, Phys. Rev. C 2 (1970) 1616–1622.
[10] W.K. Hensley, W.A. Bassett, J.R. Huizenga, Pressure dependence of the radioactive decay constant of beryllium-7, Science 181 (1973) 1164–1165.
[11] J.A. Tossell, The effects of hydrolysis and oligomerization upon the NMR shieldings of Be^{+2} and Al^{+3} species in aqueous solution, J. Magn. Reson. 135 (1998) 203–207.
[12] J.A. Tossell, Be^{2+} (aq) hydrolysis and complexation: Using calculated and experimental ^{9}Be NMR shifts to determine Be speciation in solution, Adv. Mol. Struct. Res. 6 (2000) 131–158.
[13] D.L. Bryce, R.E. Wasylishen, Beryllium-9 NMR study of solid bis(2,4-pentanedionate-O,O′) beryllium and theoretical studies of ^{9}Be electric field gradient and chemical shielding tensors. First evidence for anisotropic beryllium shielding, J. Phys. Chem. A 103 (1999) 7364–7372.
[14] J.A. Tossell, Quantum mechanical calculations of ^{23}Na NMR shieldings in silicates and aluminosilicates, Phys. Chem. Miner. 27 (1999) 70–80.
[15] B.L. Sherriff, H.D. Grundy, J.S. Hartman, F.C. Hawthorne, P. Cerny, The incorporation of alkalis in beryl: multi-nuclear MAS NMR and crystal-structure study, Can. Miner. 29 (1991) 271–285.
[16] L. Alderighi, P. Gans, S. Midollini, A. Vacca, Aqueous solution chemistry of beryllium, Adv. Inorg. Chem. 50 (2000) 109–172.
[17] F. Jensen, Introduction to Computational Chemsitry, Wiley, New York, 1999.
[18] W.J. Hehre, L. Radom, P.v.R. Schleyer, J.A. Pople, Ab Initio Molecular Orbital Theory, Wiley, New York, 1986.
[19] M.J. Frisch et al., GAUSSIAN94, Rev. B.3, Gaussian, Inc., Pittsburgh, PA, 1994.
[20] M.W. Schmidt et al., General atomic and molecular electronic structure system, J. Comput. Chem. 14 (1993) 1347–1363.
[21] J.F. Hinton, P.L. Guthrie, P. Pulay, K. Wolinski, Ab initio quantum-mechanical chemical-shift calculations for the ^{29}Si nucleus in a variety of compounds, J. Magn. Reson. A103 (1993) 188–190.
[22] T.H. Dunning, J. Chem. Phys. 55 (1971) 716–723.
[23] V. Barone, in: D.P. Chong (Ed.), Recent Advances in Density Functional Methods, Part I, World Scientific, Singapore, 1996.
[24] D.C. Palmer, CrystalMaker 3: Interactive Crystallography for MacOS, CrystalMaker Software, Bicester, 1998.
[25] H. Nakatsuji, M. Izawa, Calculation of hyperfine splitting constants with Slater-type cusp basis by the symmetry adapted cluster-configuration interaction theory, J. Chem. Phys. 91 (1989) 6205–6214.
[26] R.W.G. Wyckoff, Crystal Structures, 2nd edn., Vol. 1, Wiley, New York, 1966.
[27] R. Stahl, C. Jung, H.D. Lutz, W. Kockelmann, H. Jacobs, Kristallstrukturen und Wasserstoffbruckenbindungen bei β-$Be(OH)_2$ und ε-$Zn(OH)_2$, Z. Anorg. Allg. Chem. 624 (1998) 1130–1136.
[28] A. Tulinsky, C.R. Worthington, Basic beryllium acetate: Part II. The structure analysis, Acta Crystallogr. 12 (1959) 626–634.